PHOTOELECTRIC INJECTOR DESIGN CONSIDERATIONS*

Bruce E. Carlsten and Richard L. Sheffield
Los Alamos National Laboratory, MS H825, Los Alamos, NM 87545

Abstract

We will present an analysis for different emittance growth mechanisms for electron beams in photoelectric injectors. The mechanisms will be broken up into three groups: space-charge forces due to self-similar expansion, space-charge forces due to non-self-similar expansion (including divergences and convergences of the beam), and rf forces. We will show that some of the emittance can be eliminated downstream, particularly that of the first group. General design considerations will become clear from this analysis and a generic design will be presented. In addition, a photoelectric injector design for both the Los Alamos National Laboratory XUV FEL and a compact free-electron laser (FEL) will be used to show numerical agreement with the analysis.

Introduction

One of the most important recent improvements in electron accelerator brightness is the introduction of photoelectric injectors.[1] A photoelectric injector consists of a laser-driven cathode in an rf cavity, followed by more rf cavities that provide extremely quick acceleration to multiple MeVs. Instantaneous peak currents of hundreds of amperes to kiloamperes is possible from the cathode so further bunching is not necessary. Computer simulations of photoelectric injectors have shown very low transverse emittances, for example, normalized 90% emittances of 20 π·mm·mrad for a 20-ps, 400-A beam.[2] Typical results show that emittances are one-tenth or less than those expected from thermionic cathodes with conventional velocity bunching to obtain the same amount of peak current. Obviously, a significant reduction in emittance growth is expected with the photoelectric injector because of the removal of the long, low-voltage drift. This improvement can be easily estimated from well-known formulae for emittance growth,[3] which show the emittance grows like

$$\frac{d\varepsilon}{dz} = k/(\gamma\,\beta)^3$$

for some constant k. However, the calculated emittance using these formulae is much greater than one would expect; in fact, for a case examined later in this paper, the emittance is only one-third that predicted by the formulae from Ref. 3. In this paper, we will explain this discrepancy by showing that a different physical mechanism available for emittance reduction is possible for the photoelectric injector but not for conventional thermionic injectors. This mechanism is able to remove correlated emittance (variations in the transverse phase space correlated with longitudinal position) if there has been no substantial longitudinal mixing of the particles. In a thermionic injector, longitudinal mixing occurs because of the velocity bunching required to obtain high peak currents (>100 A), because the cathodes are only capable of producing tens of amperes instantaneous current. This longitudinal mixing effectively thermalizes the beam, removing the

correlations. Radial mixing is also undesirable but not as disastrous, as we will see later. In addition, we will show that the injector and the accelerator are intimately connected by this mechanism and cannot be separated. Thus, one should not view the injector as a separate front end of the accelerator beamline up to 10 or 20 MeV but rather as only one injector-accelerator integrated structure. For the purposes of this paper, the term injector will include the entire beamline from the cathode to the target device that the accelerated beam is meant for (in our examples, this is a free-electron laser oscillator).

In the next section we will discuss various mechanisms responsible for emittance growth. This discussion will be separated into four parts. In the first part we will review the linear space-charge emittance growth and reduction mechanism for a nonaccelerating drifting slug beam with focusing.[2] This simple model is useful because it is the only special case whose solutions provide a clear physical interpretation. In the next two parts, the effects of rf acceleration and rf focusing will be included for the linear space-charge mechanism. Finally, nonlinear space charge and nonlinear and time dependent rf effects will be accounted for. In the last section, simulations from a Los Alamos National Laboratory photoelectric injector will be presented to show numerical agreement with the analysis.

Emittance Analysis

There are four mechanisms in the injector that contribute to emittance growth:

- Linear space charge
- Nonlinear space charge
- Nonlinear time-independent rf
- Linear time-dependent rf

We will examine each of these mechanisms. From the examples in the last section of this paper, we will see that the first mechanism will dominate in general, contributing emittances three times as large as those combined from the other mechanisms. However, we will see that if there is no longitudinal mixing, we can, in principle, completely eliminate it and the resulting emittance is due primarily to a tradeoff between the second and fourth mechanisms. The first three parts in this section will examine the linear space-charge mechanism in detail; a review of previous work will be followed by introducing rf acceleration and rf focusing into the model. The last three mechanisms will be studied together in the last part.

Linear Space Charge

In this part, we will review an analysis of the linear space-charge mechanism for a drifting slug beam (given in a previous paper [2]) and obtain an expression for the beam's emittance as a function of position. We will postpone defining what we mean by linear space charge until Eq. (2); a discussion will follow.

In Fig. 1 we see a typical emittance plot as a function of distance down the linac for a typical simulation for an 8-nC, 20-ps bunch in a 1.3-GHz photoinjector. We see an immediate emittance growth to about 100 π·mm·mrad and subsequent reduction to a minimum of about 25 π·mm·mrad at a location z_f downstream. The location of z_f can be pushed far away arbitrarily; at a sufficiently high energy, there is essentially no emittance growth after that location. We will show how this emittance growth and

Normalized rms emittance (mm·mrad)

(a)

(b)
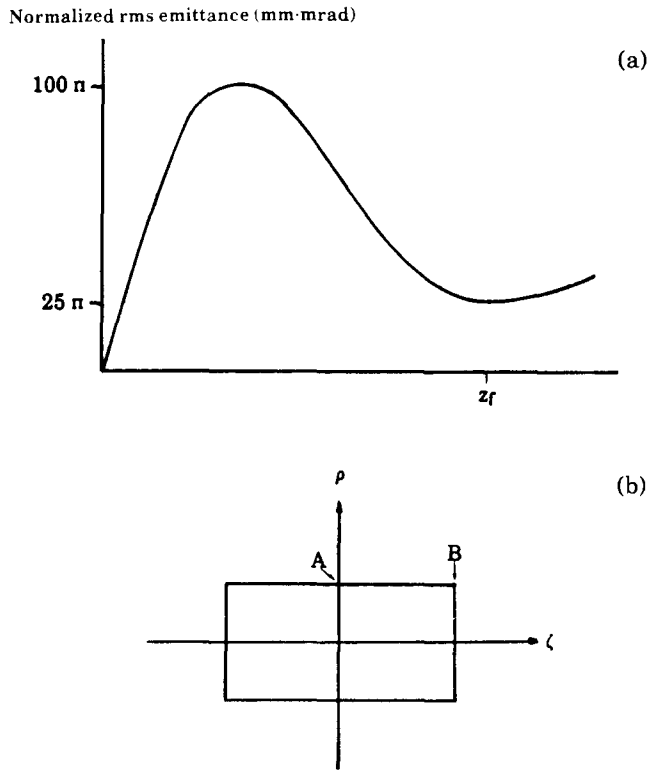
Fig. 1. (a) Typical emittance plot as a function of distance down the linac for an 8-nC, 20-ps pulse in a 1.32-GHZ photoinjector; (b) Drifting slug-beam internal coordinate system.

reduction occur with a simple model. We will study a drifting slug beam (Fig. 1); the effects of rf acceleration and rf focusing will be shown to be a variation in the definition of the normalized space-charge force $m_0\lambda$, the distances z and z_1, and the initial size and divergence of the slug. For convenience, we will also define an internal coordinate system ρ and ζ to indicate different points in the slug beam, with $\rho = r_0$ defining the initial radial size. In Fig. 1 we define points B to represent the axial edges for $\rho = r_0$ and points A to represent the center for $\rho = r_0$. We let the slug beam drift from a cathode at position $z = -z_1$ to a lens at $z = 0$ and a distance z after the lens. We have shown in the earlier paper that the lens can reduce the emittance.

First, we will examine the effect of constant space charge. We will call this the weak focusing limit. This case with zero initial beam divergence has a solution that is consistent with a well-focused beam downstream, which is not true in general. We assume the space-charge force $m_0\lambda$ (m_0 is the electron rest mass) is a function only of ρ and ζ and not of z. The edge of the beam initially at location (r_0, ζ) will obey

$$r(\zeta) = r_0 + \lambda(r_0, \zeta) z_1^2/2$$

and

$$r'(\zeta) = \lambda(r_0, \zeta) z_1$$

at the lens. If we define the focal length $1/a_L$ of the linear lens at $z = 0$ to be

$$a_L = 2 \frac{z_1 + z}{z^2}$$

then

$$\frac{r'(\rho, \zeta)}{r(\rho, \zeta)} = \frac{2(z_1 + z)}{z(z + 2z_1)}$$

at z for all positions ρ and ζ in the slug; thus, at this location, the emittance from the linear space charge has been reduced to zero.

The unnormalized rms emittance, defined as

$$\varepsilon = 2 \sqrt{<r^2><r'^2> - <rr'>^2} \quad ,$$

where the brackets refer to averages over the beam and $r' = dr/dz$, will obey

$$\varepsilon^2 = [<\lambda^2><\rho^2> - <\lambda\rho>^2][2r_0(z_1 + z) - a_L z^2 r_0]^2 \quad .$$

With the separation of the two terms, it is clear that laminarity is not required, or

$$\lambda(\rho, \zeta_0) \neq (\rho/\rho_0)\lambda(\rho_0, \zeta_0)$$

in general. However, some degree of laminarity is needed to meet the similar expansion requirement, Eq. (2). Solving for the emittance rather than a_L explicitly is superior because the solution for a_L drops out conveniently.*

To maintain similar beam expansion, we don't want the beam to expand too much or go through a crossover. In this particular example,

$$r'(\rho, \zeta) = \frac{z_1 + z}{z^2} \left[\lambda(\rho, \zeta)(z^2 - z_1^2) - 2r_0 \right] \quad .$$

Thus if $z < z_{crit}$, then the beam has a crossover before the minimum emittance position and if $z > z_{crit}$, then there is a waist before it, where we let

$$z_{crit}^2 = z_1^2 + 2r_0/\lambda \qquad (1)$$

(λ can be considered roughly constant over the slug beam). The model is most accurate for z values just slightly larger than z_{crit}. This equation is used as a guide for designing a photoelectric injector by determining the best position z_1 for lens placement. One nice feature of the boundary conditions in this case is that the minimum emittance location occurs near a waist so the beam is well focused. This is not true in general.

In addition, it was shown that if the beam expansion is similar (our earlier definition[2] for linear space charge)

$$\frac{d}{dz} \left| \frac{\lambda(\rho_1, \zeta_1)}{\lambda(\rho_2, \zeta_2)} \right| = 0 \quad , \qquad (2)$$

the analysis still holds for λ as a function of z. A solution for a_L is given by

$$a_L = \frac{\int_{-z_1}^{z} \lambda(z') dz'}{z \int_0^z \lambda(z') dz' - \int_0^z \int_{-z_1}^{z_2} \lambda(z') dz' dz_2} \quad .$$

From Eq. (2) we know that

$$\lambda(\rho, \zeta, z) = k(\rho, \zeta)\lambda(z) \quad ,$$

*Private communication, M. E. Jones, Los Alamos National Laboratory

where all the differences in the space charge between particles is in the k (ρ, ζ, z) term. Allowing initial divergence r_0' at $z = -z_1$, we can write the emittance as

$$\varepsilon^2 = (<k^2><\rho^2> - <k\rho>^2)\left\{(r_0 + r_0' z_1)\int_{-z_1}^{z}\lambda(z')\,dz'\right.$$

$$-r_0'\left[\int_0^z dz_2\int_0^{z_2}\lambda(z')\,dz' + \int_{-z_1}^0 dz_2\int_{-z_1}^{z_2}\lambda(z')\,dz'\right] \qquad (3)$$

$$+ r_0' z\int_0^z\lambda(z')\,dz$$

$$\left.-a_L(r_0 + r_0' z_1)\left[z\int_p^z\lambda(z')\,dz' - \int_0^z dz_2\int_0^{z_2}\lambda(z')\,dz'\right]\right\}^2 \quad .$$

Again, it is easy to get an expression for a_L; however, because in general $\lambda(z)$ depends on a_L, it may be difficult to derive an explicit solution for a_L. It is useful to remember that the $(<k^2><\rho^2> - <k\rho>^2)$ term is a constant independent of position.

Linear Space Charge with RF Acceleration

With rf acceleration, Eq. (3) changes. The beam frame time t_b is related to the laboratory longitudinal position by

$$dz = (\gamma\beta c)\,dt_b \quad ,$$

and the beam and laboratory space-charge forces by

$$\lambda = \lambda_b(\gamma\beta c) \quad .$$

We can rewrite Eq. (3) as

$$\varepsilon^2 = \left(<\lambda^2><\rho^2> - <\lambda\rho>^2\right)\left(\left[(r_0 + r_0'\int_{-z_1}^0\frac{dz}{\gamma(z)\beta(z)}\right]\right.$$

$$\cdot\int_{-z_1}^z\frac{\lambda(z')\,dz'}{[\gamma(z')\beta(z')]^2} - r_0'\left\{\int_0^z\frac{dz_2}{\gamma(z_2)\beta(z_2)}\int_0^{z_2}\frac{\lambda(z')\,dz'}{[\gamma(z')\beta(z')]^2}\right.$$

$$\left.+\int_{-z_1}^0\frac{dz_2}{\gamma(z_2)\beta(z_2)}\int_{-z_1}^{z_2}\frac{\lambda(z')\,dz'}{[\gamma(z')\beta(z')]^2}\right\}$$

$$+ r_0'\int_0^z\frac{dz}{\gamma(z)\beta(z)}\int_0^z\frac{\lambda(z')\,dz'}{[\gamma(z')\beta'(z')]^2}$$

$$- a_L\left[r_0 + r_0'\int_{-z_1}^0\frac{dz}{\gamma(z)\beta(z)}\right]\left\{\int_0^z\frac{dz}{\gamma(z)\beta(z)}\int_0^z\frac{\lambda(z')\,dz'}{[\gamma(z')\beta'(z')]^2}\right.$$

$$\left.\left.-\int_0^z\frac{dz_2}{\gamma(z_2)\beta(z_2)}\int_0^z\frac{\lambda(z')\,dz'}{[\gamma(z')\beta'(z')]^2}\right\}\right)^2 \quad . \qquad (4)$$

Eq. (4) can be integrated with a computer code if the form of the accelerating gradient is known. At this point, it would be nice if with λ constant and $r_0' = 0$, we could get an expression for z similar to Eq. (1), which would give us guidance in placing our lens. Using $\gamma\beta = 1 + H(z + z_1) \equiv u$ for some constant H (which is not constant gradient, but does lead to equations we can solve), then

$$\gamma\beta r' = \left\{\frac{(1 - 1/u)H}{1/u_0 - [1 + \log(u/u_0)]/u}\right\}$$

$$\cdot\left[\left(\frac{\lambda k}{H^2}\right)(1 - 1/u)\left(1 - \log u_0\right) - \frac{1}{u}\log u - r_0\right]$$

at the minimum emittance location, with $u_0 = 1 + Hz_1$. The resulting equation analogous to Eq. (1) is

$$\log u_0 = 1 - \frac{\log u + ur_0 H^2/(\lambda k)}{u - 1} \quad .$$

Linear Space Charge with RF Focusing

If the beam expansion is sufficiently self-similar, then we can write an explicit solution for a_L. If

$$r'' = k(\rho, \zeta)\lambda(z) - (\rho/\rho_0)a(z) \quad , \qquad (5)$$

then

$$a_L = N/M \quad ,$$

where

$$N = \left[r_0 - \int_{-z_1}^z\int_{-z_1}^{z_2}a(z')\,dz'\,dz_2\right]\left[\int_{-z_1}^z\lambda(z')\,dz'\right]$$

$$+\left[\int_{-z_1}^z\int_{-z_1}^{z_2}\lambda(z')\,dz'\,dz_2 + \int_{-z_1}^0\lambda(z')\,dz\right]\left[\int_{-z_1}^z a(z')\,dz'\right]$$

and

$$M = r_0\left[z\int_0^z\lambda(z')\,dz' - \int_0^z\int_{-z_1}^{z_2}\lambda(z')\,dz'\,dz_2\right]$$

$$+\int_{-z_1}^0\int_{-z_1}^z a(z')\,dz'\,dz\left[\int_{-z_1}^{z_2}\int_{-z_1}^z\lambda(z')\,dz'\,dz\right]$$

$$+z\int_{-z_1}^0\lambda(z')\,dz'\right] + z\left[\int_{-z_1}^0\int_{-z_1}^{z_2}\lambda(z')\,dz'\,dz_2\int_{-z_1}^z\right.$$

$$a(z')\,dz' - \int_0^z\int_{-z_1}^{z_2}a(z')\,dz'\,dz_2\int_{z_1}^0\lambda(z')\,dz'$$

$$\left.-\int_{-z_1}^0\int_{-z_1}^{z_2}a(z')\,dz'\,dz_2\int_{-z_1}^z\lambda(z')\,dz'\right] \quad ,$$

and the emittance is

$$\varepsilon^2 = (<k^2><\rho^2> - <k\rho>^2)(N - a_L M)^2 \quad .$$

A solution still exists if we relax the similarity restraint for the focus, although the solution cannot be written explicitly. We start with

$$r'' = \lambda - ar$$

with initial boundary conditions $r = r_1$, and $r' = r_1'$ at $z = 0$. Then

$$(\lambda - 2ar) = (\lambda - 2ar_1)\cos(\sqrt{a}\,z) - 2r_1'\sqrt{a}\sin(\sqrt{a}\,z)$$

and

$$2ar' = (\lambda - 2ar_1)\sqrt{a}\sin(\sqrt{a}\,z) + 2r_1' a\cos(\sqrt{a}\,z) \quad .$$

Because λ still occurs linearly in these equations, we know a solution for a_L exists for minimum emittance. If we assume $a(z)$ is piecewise constant, we can write a computer code to iterate r and r' over regions of constant focusing. Under certain conditions, the addition of the rf focusing will effectively change the initial conditions z_1, r_0, and r_0' for the nonfocusing case. For example, if we have a beam with constant focusing a for a distance z_2, followed by a drift of z_1 to a lens with focal length $1/a_L$ and with a final drift z, the earlier analysis holds if we replace

r_0 by $r_0 \cos(\sqrt{a}\, z_2) + r_0' \sin(\sqrt{a}\, z_2)/\sqrt{a}$,

r_0' by $r_0' \cos(\sqrt{a}\, z_2) - r_0 \sqrt{a} \sin(\sqrt{a}\, z_2)$,

and

$$z_1 \ \text{by} \ z_1 + \frac{\sin(\sqrt{a}\, z_2)}{2\sqrt{a}}$$

for sufficiently small $(\sqrt{a}\, z_2)$ [the error is of order $(\sqrt{a}\, z_2)^4$].

Other Mechanisms

Nonlinear Space Charge

Nonlinear space-charge effects cannot in general be removed. Thus for the weak focusing limit, the criterium of Eq. (1) must be used to minimize the non-similar beam expansion. As you will see in the last section with this criterium, the nonlinear space charge is still not negligible. In addition to non-self-similar beam expansion, nonlinear space charge can occur from beam divergences and convergences. With a beam angle of θ, the emittance grows like

$$\varepsilon = 2\sqrt{2}\, \lambda\, \theta\, z \sqrt{\frac{L^2}{24} + \frac{\theta^2}{r_0^2}\frac{L^4}{80}}$$

for a drift of length z and a bunch of length L. The first term is a constant for any angle, but the second term grows for larger θ.

Nonlinear Time-Independent RF Fields

This term refers to the nonlinear component in the rf fields, i.e., the component that deviates from

$$E_r(r,z) = E_0(z)\, r \cos(wt + \phi) \ . \tag{6}$$

An earlier work has calculated cavity shapes for linear rf fields for sufficiently low enough frequencies that the electrostatic solution can be used.[4] An extension to electromagnetic fields is possible and necessary; at 1.3 GHz, the nonlinearity of the fields contribute something like 15 n·mm·mrad to the normalized 90% emittance.

Linear Time-Dependent RF Fields

For one of the cases we will consider in the next section, the emittance of 15 n·mm·mrad arises from a combination of 11 n from the nonlinear space-charge effect and 11 n from the linear time-dependent rf fields for a pulse of 20 ps. This last effect occurs from the time dependency of the rf fields. We assume the rf fields obey Eq. (6). Then the form of the emittance resulting from the time dependency is

$$\varepsilon \sim E_0 r^2 L \ ,$$

where r is the radius of the beam, and L is its length.[5] The physical size of the beam can be reduced to make these effects smaller until the nonlinear space-charge forces appear. With zero charge in the beam, it is possible to eliminate this effect with a third-harmonic cavity following each linac section because there will be no radial mixing. However, with space charge, the radial mixing destroys the correlation before the third-harmonic cavity. To reduce this effect with space charge, either a third-harmonic component must be introduced into each of the first cavities or the constant E_0 must be reduced for each one. The constant E_0 can be reduced by proper selection of the parameters μ and ψ in the linear field solution extension of Ref. 4 for electromagnetic fields.

A second effect from the time-dependent nature of the rf fields is the time-dependent acceleration of different particles. If the pulse is sufficiently long so that different particles of the beam bunch have different relativistic velocities when they encounter the lens, then the linear space-charge term will not be completely removed. This effect is aggravated if the lens position is near the first cavity. There the different energies between particles can be quite large. This effect can be as big as 150 n·mm·mrad for a 50-ps pulse with 20 nC for a 1.3-GHz structure. One way to reduce this effect is to introduce long drift regions that bring the lens position downstream from the first cavity so that the energy spread will be a lower percentage.

Simulations of Generic Design

For a generic design, we will use a photoelectric injector with a magnetic lens. There is a bucking coil so that there is no flux at the cathode. The four variables in the design are the

- accelerating gradient profile,
- initial cathode size,
- initial beam divergence, and the
- rf focusing in the first cavity.

We assume the magnetic field profile of the lens enters only in the form $\int B_z\, dz/\gamma$.

Operating at 1.3 GHz, we select gradients of 26 MeV/m for the first two cells and 8 MeV/m for the remainder, grouping 15 cells in each linac tank. The selected n-mode structure with linear rf fields for all cavities has no graded beta section. The first cavity is half the size of the other cavities; therefore, the cathode is planar ($r_0' = 0$), and there is no rf focusing in the first cavity.

We see in Fig. 2 the effects of varying the lens position for the above conditions. Figure 2a shows that for the correct lens position, the emittance minimum and the beam focus occur at the same location downstream. The asymmetric shape of the emittance curve is caused by acceleration of the electrons. If we move the lens upstream and vary its strength so that the emittance minimum occurs at that same location, we observe a beam waist before the emittance minimum (Fig. 2b), which is in agreement with Eq. (1). If we move the lens downstream and vary its strength, the emittance minimum now occurs before a beam crossover (Fig. 2c). Although Eq. (1) indicates that a beam crossover occurs before the emittance minimum, we were forced to decrease the strength of the lens because there is unacceptable emittance growth from the nonsimilar beam compression. Because the lens strength is incorrect for this case, we expect a larger emittance than in the other two cases. However, this effect is minor compared to the additional emittance growth from the rf effects and nonsimilar beam expansion as the beam expands to a larger size before it reaches the lens position further downstream.

Emittance (mm·mrad)   Radius (cm)
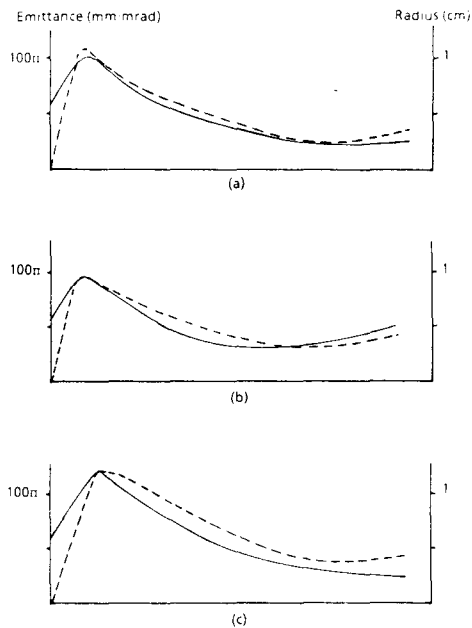
Fig. 2. Radius (solid line) and 90% normalized emittance (dashed line) of the beam as a function of longitudinal position for (a) correct lens placement, (b) lens too near cathode, and (c) lens too far from cathode. Cathode position is at the far left edge of plot.

Conclusion

A photoelectric injector design analysis has been presented. This analysis includes electrostatic and rf focusing and acceleration. The emittance growth from the dominant mechanism has been shown to be eliminated with a simple lens configuration, leaving only a small residual emittance resulting from the other mechanisms. The photoelectric injector with a single lens can be used as a generic design. Additional lenses are included in the electrostatic focusing term. Computer simulations of this design show good agreement with the analysis.

Acknowledgment

The authors wish to acknowledge the helpful discussions held with Lloyd Young and Michael Jones.

References

1. J. S. Fraser, R. L. Sheffield, E. R. Gray, P. M. Giles, R. W. Springer, and V. A. Loebs, "Photocathodes in Accelerator Applications," Proc. 1987 IEEE Particle Accelerator Conf., IEEE Catalog No. 87CH2387-9, 1319 (1987).
2. B. E. Carlsten, "New Photoelectric Injector Design for the Los Alamos
    National Laboratory XUV FEL Accelerator," 10th FEL Conf., Jerusalem, August 29–September 2, 1988.
3. M. E. Jones and B. E. Carlsten, "Space-Charge Induced Emittance Growth in the Transport of High-Brightness Electron Beams," Proc. 1987 IEEE Particle Accelerator Conference, IEEE Catalog No. 87CH2387-9, 1319 (1987).
4. M. E. Jones and W. Peter, "Particle-in-Cell Simulations of the Lasertron," IEEE Trans. Nucl. Sci. 32 (5), 1794 (1985).
5. M. E. Jones and W. Peter, "Theory and Simulation of High-Brightness Electron Beam Production from Laser-Irradiated Photocathodes in the Presence of dc and rf Electric Fields," Los Alamos National Laboratory document LA-UR-86-1941, Proc. 6th Int. Conf. on High-Power Particle Beams, Kobe, Japan, June 1986, to be published.